COBEM UBERLÂNDIA 2019

ABCM Associação Brasileira de Engenharia e Ciências Mecânicas

25th ABCM International Congress of Mechanical Engineering
October 20-25, 2019, Uberlândia, MG, Brazil

COB-2019-1619
MODEL SCALE PROPELLER TIP VORTEX ASSESSMENT USING VORTEX IDENTIFICATION METHODS

Fillipe Rocha Esteves
University of São Paulo - Dept. of Naval Architecture and Ocean Engineering. 2231, Prof. Mello Moraes Av. - Cidade Universitária - São Paulo - SP - Brazil
Institute for Technological Research Foundation (FIPT)
fillipe.esteves@usp.br

João Lucas Dozzi Dantas
Institute for Technological Research. 532, Prof. Almeida Prado - Cidade Universitária - São Paulo - SP - Brazil
jdantas@ipt.br

Abstract. *The investigation of vortex distribution pattern is an important issue in marine propeller design, as it may lead to improvements in performance and hydro-acoustics properties. The velocity field and its derivatives obtained from CFD simulations of a marine propeller designed to the DARPA Suboff wake were analyzed in this work. The rotational field in the propeller wake was investigated for flow velocities corresponding to advance coefficients between 0.2 and 1.2, including the operation condition. The λ_2 and Q fields were computed and vortex centers found by two vortex identification methods, enabling the quantitative comparison between different velocity conditions and analysis methods. The proposed post-processing method is capable of analyzing both experimental and numerical data.*

Keywords: *tip vortex, vortex dynamics, vortex identification, DARPA Suboff*

1. INTRODUCTION

The employment of singular geometries on marine propeller design, as high skew and blade's low aspect ratio, is an usual alternative to mitigate undesirable phenomena such as vibration, noise and efficiency decay during the propeller operation. However, complex shapes lead to strong three-dimensional effects on the propeller wake. These effects can be observed on experimental tests or CFD simulations as vortical structures and are commonly organized according to it's generation mechanism. Felli and Falchi (2018) listed five types of vortex structures: tip, trailing, shed, hub and junction vortex.

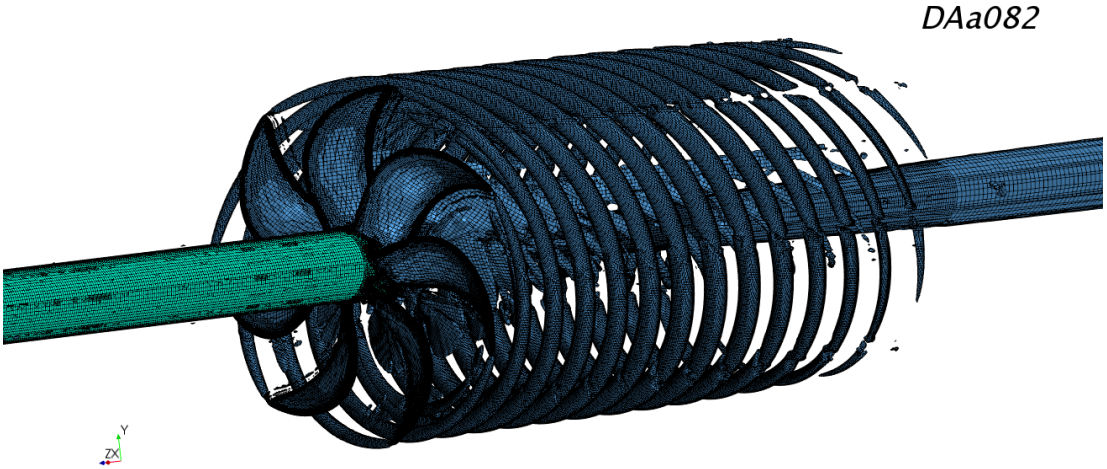

Figure 1: Seven-blade propeller with tip and hub vortex representation using Q-Criterion

Also observed on other winglike bodies, tip vortex are shed because of the pressure gradient between suction and pressure sides of the propeller blades. On tip region, this gradient generates a pressure side to suction side flow that

introduces rotational movement to the fluid. In marine applications, the reduction of water's vapor pressure inside tip vortex cores may causes cavitation and noise problems, as pointed by Souders and Platzer (1981) and Sbragio (1996). Aiming to investigate the tip vortex topology shedded from a 7-bladed propeller, Silva Jr *et al.* (2019) performed open water tests on the Institute for Technological Research's Cavitation Tunnel, considering the uncertainty and blockage effects correction. The chosen model was an 1:1.588 scaled version of the Mod5 propeller. The model was designed by Sbragio (1995) to the DARPA Suboff wake, applying the Lifting Line Theory (LLT) and concomitantly analyzed with Lifting Surface Theory (LST). Its performance was predicted on Computational Fluid Dynamics software by Esteves *et al.* (2018). All the research effort is focused on the development of new techniques that support new propeller's designs, with both performance and hydro-acoustics requirements.

Results measured by Silva Jr *et al.* (2019) on Cavitation Tunnel using Particle Image Velocimeter (PIV) were taken as a 99 frames phase-averaged image and compared to scalar and vector fields obtained on section planes of CFD simulations, positioned in the same reference frame of the PIV measurement grid. The numerical solver used Reynolds-Averaged Navier-Stokes equations with $K-\omega\ SST$ turbulence model.

The present methodology aims to define a post processing algorithm, necessary to more accurately compare the tip vortex topology on experimental and numerical results. This investigation was conducted making use of the velocity vector field and its derivatives, obtained via CFD simulation and monitored on a section plane of the fluid domain.

There are applications of vortex analysis in multiple flow studies: aeronautics, civil aerodynamics (bridges and buildings, for example), atmospheric or oceanographic applications, internal flows and so on. The algorithm also may be used to other propeller vortex mechanism's analysis on future work.

2. KINEMATICS OF MOTION

Adopting the continuum hypothesis, the derivation of the fundamental equations of physics (conservation of mass, energy and momentum) become valid on the entire media. An useful way to derive these equations is the differential (or field) approach, that applies these basic principles to infinitesimal volume elements. The continuum velocity field tensor can be decomposed into symmetric and skew-symmetric tensors. The first term of equation 1 is the rate of deformation tensor S_{ij} (symmetric) and the second term is the rate of rotation tensor Ω_{ij} (skew-symmetric).

$$D_{ij} = \frac{1}{2}\left(\frac{\partial v_i}{\partial x_j} + \frac{\partial v_j}{\partial x_i}\right) + \frac{1}{2}\left(\frac{\partial v_i}{\partial x_j} - \frac{\partial v_j}{\partial x_i}\right) \tag{1}$$

Second part of the equation 1 is directly associated to the scope of this research, once it is equal to half of the fluid vorticity $\boldsymbol{\omega} = 2\Omega_{ij}$. However, some important scalar fields in the vortex analysis, such as Q-Criterion, Δ-Criterion and λ-Criterion, give the relationship between the two terms of the equation's right side, S_{ij} and Ω_{ij}. Vorticity can also be related to the velocity field by means of the equation 2:

$$\boldsymbol{\omega} = \nabla \times \mathbf{V} = e_{ijk} u_{k'j} \boldsymbol{e_i} \tag{2}$$

3. VORTEX IDENTIFICATION METHODS

Many algorithms for vortex identification were developed in literature, from the velocity field or its derivatives $\boldsymbol{D}$ and $\boldsymbol{R}$: Lugt and Gollub (1985) proposed the identification of closed or spiralling streamlines as vortex structures; Banks and Singer (1995) adopted a search for pressure local minimum on the axis of swirling motion; Jeong and Hussain (1995) defined their criterion from the velocity gradient tensor; Lesieur *et al.* (2000) used the vorticity maxima; Kopp *et al.* (2000) and Pemberton *et al.* (2002) used statistical methods for vortex identification. A compilation of these methods and the criteria obtained from them can be seen in Holmén (2012).

This work focuses on non-statistical methods, in which it is possible to manipulate an arbitrary velocity vector field in order to obtain the values of different vortex criteria to each grid cell. Raw data is obtained from CFD or PIV experimental measurements and, after post-processing, the center and outer limits of vortex structures are identified. As mentioned previously, some criteria use derivatives of the velocity field that were calculated by a symmetric difference quotient, obtained from equation 3:

$$f'(x) = \frac{f(x+h) - f(x-h)}{2h} \tag{3}$$

In which $f'(x)$ is the partial derivative of $f(x)$ in respect to x and h is the distance between two cell's centers. Methods that consider the pressure minimum and velocity gradient tensor, namely the Q-criterion and λ_2-criterion, where employed in this study. In the following subsections a brief introduction to these methods is presented.

3.1 Pressure Minimum

In a three-dimensional space, elongated low-pressure regions often indicate vortex cores in turbulent flows. Considering the helical shape of tip vortex, this low pressure region crosses the lateral section plane above and below de symmetry line, alternately. Each region intersection presents a local minimum on the valley of pressure function, that is considered the center of vortex spiral at the section plane. Having the cell size as a precision limiter for the vortex center identification, the minimum pressure point can be identified as the center of the minimum pressure cell in CFD grid.

3.2 Velocity Gradient Tensor

From Galilean invariant hypothesis, the characteristic equation of the gradient tensor Δv is used to classify the local streamline pattern around a critical point.

$$\lambda^3 + P\lambda^2 + Q\lambda + R = 0 \tag{4}$$

Where P, Q and R are the three invariants of the velocity gradient tensor. Using the decomposition into symmetric and skew-symmetric parts these invariants can be expressed as:

$$P = -tr(\boldsymbol{D}) \tag{5}$$

$$Q = \frac{1}{2}(tr(\boldsymbol{D})^2 - tr(\boldsymbol{D}^2) = \frac{1}{2}||\boldsymbol{\Omega}||^2 - ||\boldsymbol{S}||^2 \tag{6}$$

$$R = -det(\boldsymbol{D}) \tag{7}$$

The Q-criterion represents a "connected fluid region with positive second invariant of ∇v", according to Jeong and Hussain (1995).This definition states that, from equation 6, the second invariant Q is positive on the regions where the rotation rate magnitude is greater than the magnitude of rate of strain.
The idea behind λ_2 definition is that by discarding the unsteady straining and viscous effects, the existence of a pressure minimum may better indicate a vortex core. Taking the gradient of the Navier-Stokes equations, follows equation 8:

$$a_{ij} = -\frac{1}{\rho}p_{ij} + \nu u_{i,jkk'} \tag{8}$$

Where a_{ij} is the acceleration gradient and p_{ij} is symmetric. The acceleration gradient a_{ij} can be decomposed in a symmetric (first term) and a skew-symmetric part (second term), as shown in equation 9:

$$a_{ij} = \left[\frac{DS_{ij}}{Dt} + \Omega_{ik}\Omega_{kj} + S_{ik}S_{kj}\right] + \left[\frac{D\Omega_{ij}}{Dt} + \Omega_{ik}Skj + S_{ik}\Omega_{kj}\right] \tag{9}$$

Combining equations 8 and 9, unsteady straining and viscous effects must be neglected on the symmetric part of the acceleration gradient. The result of this manipulation is the equation 10:

$$\Omega_{ik}\Omega_{kj} + S_{ik}S_{kj} = -\frac{1}{\rho}p_{ij} \tag{10}$$

Information on extreme local values of pressure is contained in the Hessian of pressure, so the definition of the vortex core in λ_2-criterion is "a connected region with two negative eigenvalues of $S^2 + \Omega^2$", determining the local pressure minimum. Since $S^2 + \Omega^2$ is symmetric it has real eigenvalues only, and by ordering the eigenvalues $\lambda_1 \geq \lambda_2 \geq \lambda_3$ the definition becomes equivalent to requiring that $\lambda_2 < 0$. The Q definition does not properly represent the vortex geometry, while the λ_2 definition reveals the entire vortex core geometry.

λ_1	λ_2	λ_3	$\sum \lambda_i$	Negative λ_2	Positive Q
+	-	-	-	vortex core	vortex core
+	-	-	+	vortex core	not vortex core
+	+	-	-	not vortex core	vortex core
+	+	+	+	not vortex core	not vortex core

Table 1: Possible choices of eigenvalues and the differences of the definitions based on positive Q and on negative λ_2

4. PROPELLER ASSESSMENT

4.1 Numerical Model

A three-dimensional unstructured mesh was generated containing 12.14M of cells and four refining regions: tip vortex region, boss cap and two different sizes on propeller wake. In order to achieve Wall Y+ near to one on the propeller surface, a prism layer with 25 percent growth from the near wall element was built, with first element thickness equal to 2.5 e^{-6} m. The chosen turbulence model was the $k-\omega$ SST, for which the vortex identification methods were performed. Convergence and mesh independence were previously investigated, adopting a stopping criteria that requires simultaneously a maximum difference of 1E-5 in K_T (Thrust Coefficient) monitor and 1E-6 for K_Q (Torque Coefficient), in the last 1000 iterations. This approach ensures that convergence uncertainty is smaller than the mesh uncertainty. Propeller rotation was fixed in 1008 RPM for all simulations. In addition to the K_T and K_Q monitors, the vector velocity field and scalar fields λ_2 and Q on the propeller wake were extracted in order to continue the tip vortex mechanism study.

4.2 Vortex Identification

A plane section, defined by the blade tip and propeller symmetry axis, was created from three-dimensional domain in CFD simulations. The mesh refinement was crucial to achieve a better resolution of the tip vortex region, requiring a minimum of 20 elements inside the vortex core. Velocity vector field is obtained to each cell and treated to subtract the advance velocity imposed to the flow, in longitudinal direction. The advance velocity represents the initial condition on velocity inlet of the numerical fluid domain, disregarding disturbances due to the action of the propeller. By this deduction, a predominantly rotational flow in the tip vortex region can be verified, as can be seen in figure 2, that shows this deducted velocity field. This close up figure reveals the vortex shedding on the blade tip and the region highlighted is a Q-Criterion isosurface of $500/s$. It can be noticed the flow rotational topology with zero velocity at the center of the vortical structure.

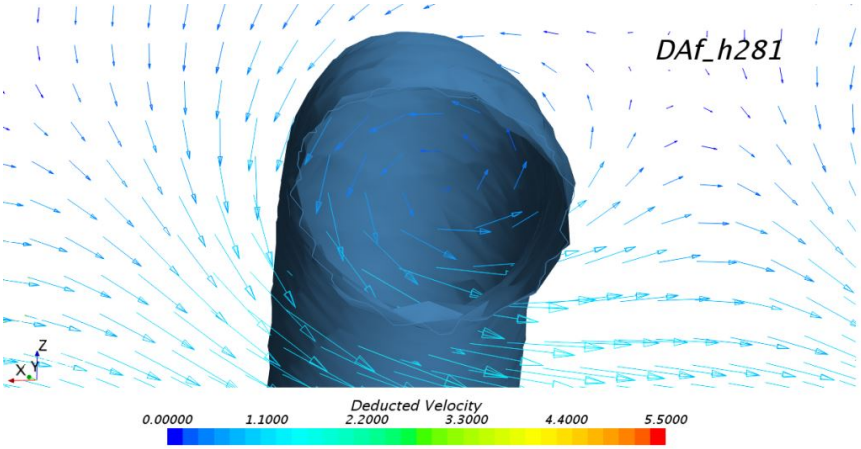

Figure 2: First helical structure on the blade tip and velocity vector field subtracting the advance velocity from longitudinal coordinates

The scalar quantities on the plane section were extracted in tabular form so that the field could be analyzed in Matlab® code in order to perform the vortex identification algorithm in the two-dimensional domain. Results were compared in 12 cases, varying the advance coefficient J from 0.2 to 1.2, with a 0.1 spacing, and the operation condition J=0.9194. To each advance coefficient, i.e., the different advance velocities, the center of the vortex core was identified using distinct approaches.

The first vortex center identification approach followed the idea of search for local minimum in the pressure field. However, its order of magnitude, as well as in other scalar fields of interest, is much higher on boss cap wake and near the blade surface. This way, it was necessary to preselect x and z coordinates wherein only the section of tip vortex cores must appear. In these regions, then, a search was conducted by the first five pressure local minima.

The other way to identify the vortex center is using the velocity field directly. By deducing the advance velocity from longitudinal component of the velocity field, the resulting vectors evidence a rotational topology around the vortex center, as discussed previously. By finding the cell that presents the minimum deducted velocity magnitude, its possible to infer the vortex center. Again, it was necessary to preselect the probable coordinates for center's search, once there are regions of velocity local minima between the vortex cores.

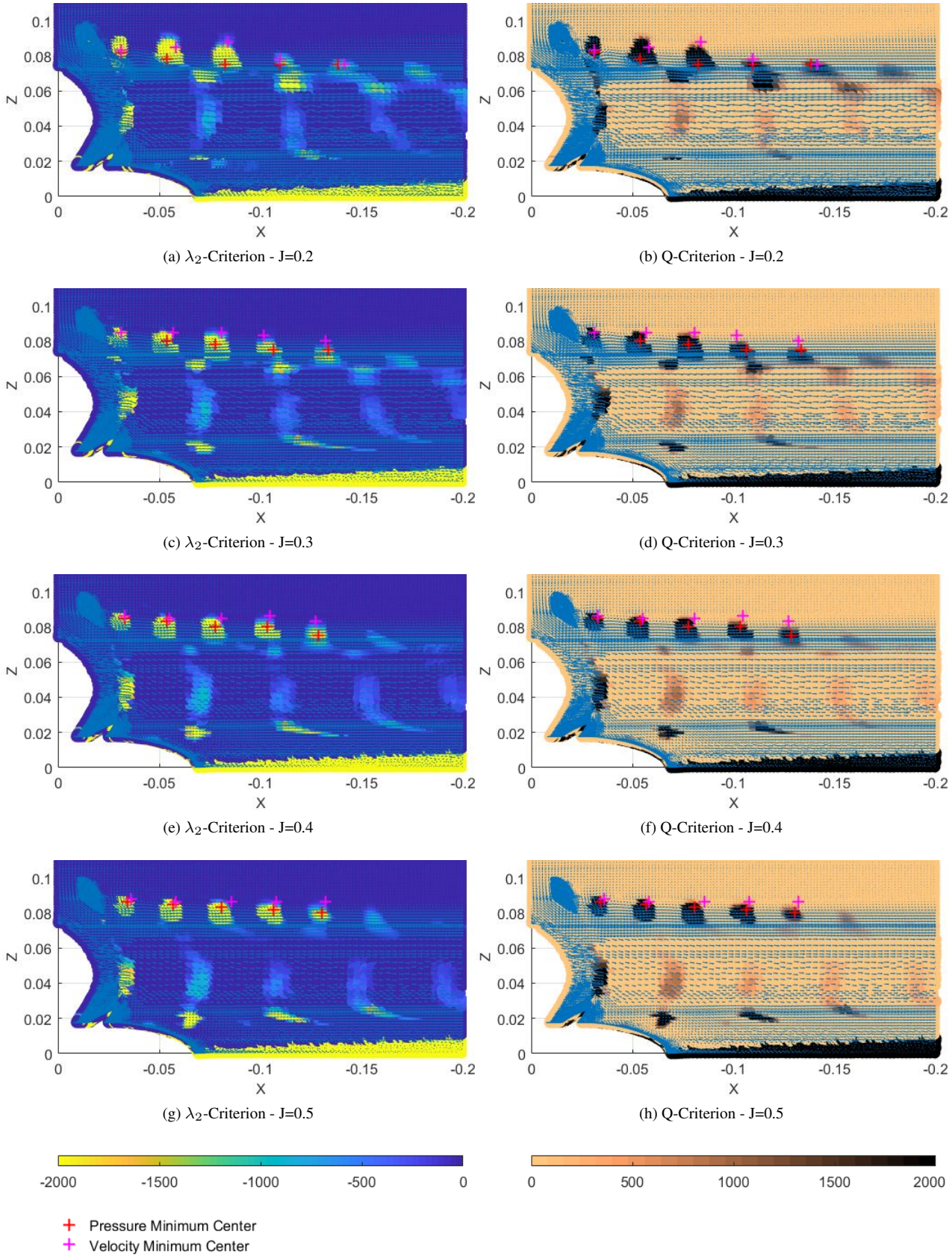

(a) λ_2-Criterion - J=0.2

(b) Q-Criterion - J=0.2

(c) λ_2-Criterion - J=0.3

(d) Q-Criterion - J=0.3

(e) λ_2-Criterion - J=0.4

(f) Q-Criterion - J=0.4

(g) λ_2-Criterion - J=0.5

(h) Q-Criterion - J=0.5

Figure 3: Computed scalar fields λ_2-Criterion and Q-Criterion to advance coefficients from 0.2 to 0.5

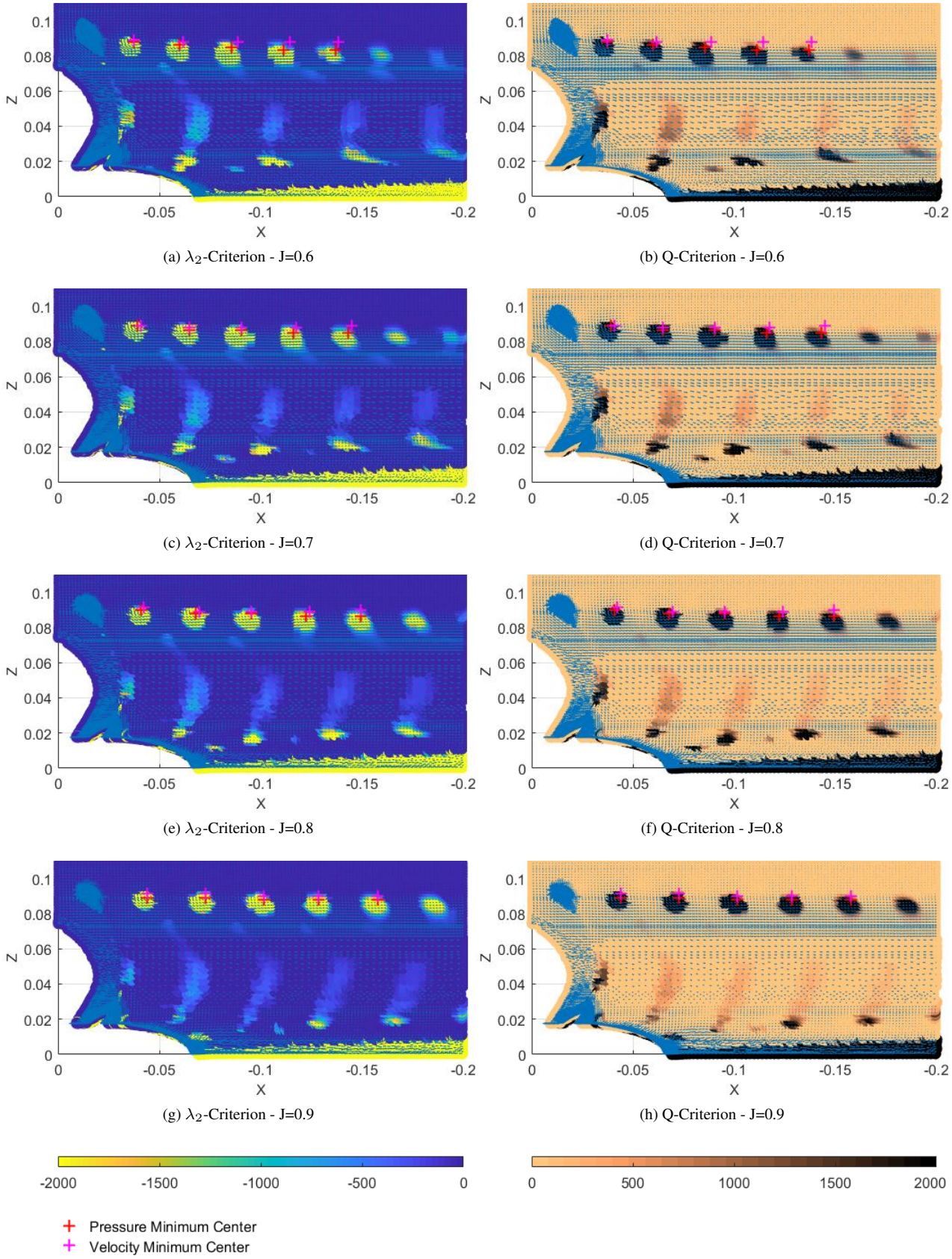

(a) λ_2-Criterion - J=0.6

(b) Q-Criterion - J=0.6

(c) λ_2-Criterion - J=0.7

(d) Q-Criterion - J=0.7

(e) λ_2-Criterion - J=0.8

(f) Q-Criterion - J=0.8

(g) λ_2-Criterion - J=0.9

(h) Q-Criterion - J=0.9

Figure 4: Computed scalar fields λ_2-Criterion and Q-Criterion to advance coefficients from 0.6 to 0.9

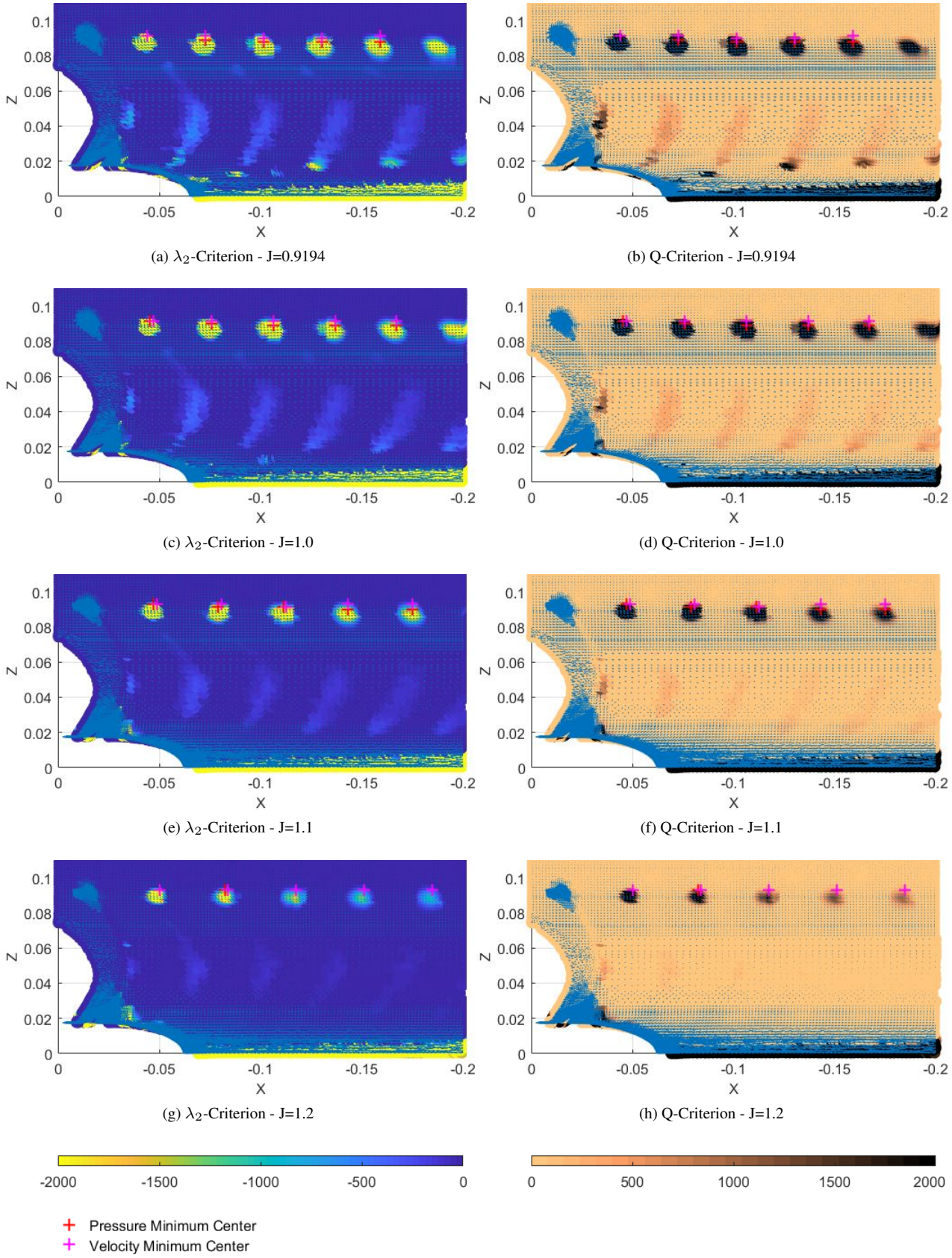

(a) λ_2-Criterion - J=0.9194

(b) Q-Criterion - J=0.9194

(c) λ_2-Criterion - J=1.0

(d) Q-Criterion - J=1.0

(e) λ_2-Criterion - J=1.1

(f) Q-Criterion - J=1.1

(g) λ_2-Criterion - J=1.2

(h) Q-Criterion - J=1.2

Figure 5: Computed scalar fields λ_2-Criterion and Q-Criterion to advance coefficients from 0.9194 to 1.2

Figures 3, 4 and 5 give a comparison of λ_2 (left) and Q (right) fields for each simulated advance coefficient. All similar graphs are in the same scale: from $-2000/s$ to $0/s$ for λ_2 and from $0/s$ to $2000/s$ for Q. Its important to note that X-axis is positively oriented to what would be an advance forward in the ship's reference, that results negative coordinates as the vortex develops and moves away from the propeller. The origin of coordinate system is in the radial symmetry line and longitudinally in the center of the propeller hub. Table 2 gives a relation of presented graphs and how they are organized throughout the figures.

J = $\frac{Va}{nD}$	0.2	0.3	0.4	0.5	0.6	0.7	0.8	0.9	0.9194	1.0	1.1	1.2
λ_2	3.a	3.c	3.e	3.g	4.a	4.c	4.e	4.g	5.a	5.c	5.e	5.g
Q	3.b	3.d	3.f	3.h	4.b	4.d	4.f	4.h	5.b	5.d	5.f	5.h

Table 2: Relation of graph's figures for scalar quantities in different advance coefficients

More elevated values of both λ_2 and Q fields are perceived on the boss cap wake, reaching about $50000/s$ in absolute magnitudes. On the other hand, trailing vortex absolute magnitudes stay between $0/s$ and $500/s$. These different scales in regions that arise from different generation mechanisms favor the identification algorithm.

Were also plotted in this graph comparison: the deduced velocity field in small blue arrows; and the vortex center positions identified by the minimum pressure algorithm (red crosses) and those found by the minimum deducted velocity algorithm (magenta crosses).

The vortex core center identification made possible the development of a quantitative study of the wake characteristics. The difference between the longitudinal coordinates x of a center and its next center was calculated as the spiral pitch, while the vertical coordinate z of each vortex was defined as the center radius.

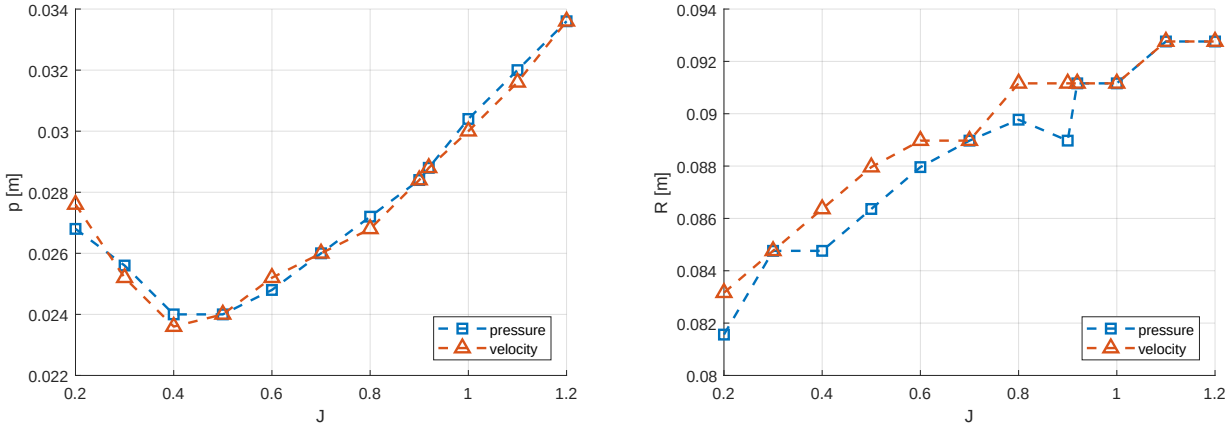

Figure 6: Quantitative results for vortex center identification: mean pitch (left) and mean radius (right) obtained from the first five centers as function of the advance coefficient

To each advance coefficient, the mean values of both pitch and radius were calculated using the data relative to the corresponding five first centers and results are plotted in figure 6. On the left side, the mean pitch values obtained from pressure minimum centers (blue squares) and from deducted velocity minimum centers (orange triangles) are compared. On the right, the same comparison is done for mean radius values. For both cases, although calculations are limited to mesh definition, the pressure and velocity values presented good correlation. Mesh discretization may slightly affect the position of vortex centers.

It was observed that pitch remains constant along the first five centers for faster flows, i.e., flows with higher advance coefficients. For $J < 0.4$ it is possible to note that the region of instability near the propeller longs for the first three vortex cores. The change on these patterns results in a growing pitch that becomes stable only from the third vortex onwards.The pitch evolution among the five studied vortex centers is shown in the figure 7, considering the twelve cases with different advance coefficients and the pressure minimum approach.

Varying the advance coefficient, the radii of the first five vortex centers and their longitudinal positions either change. Figure 8 shows the vortex center radii as function of x coordinate and advance coefficient. These results were explored using the pressure minimum approach. Fixing the advance coefficient, a change in radius between the five first centers occurs. From the graph, its noticeable that the changing rate is higher for slower flows, what indicates a similarity to pitch results.

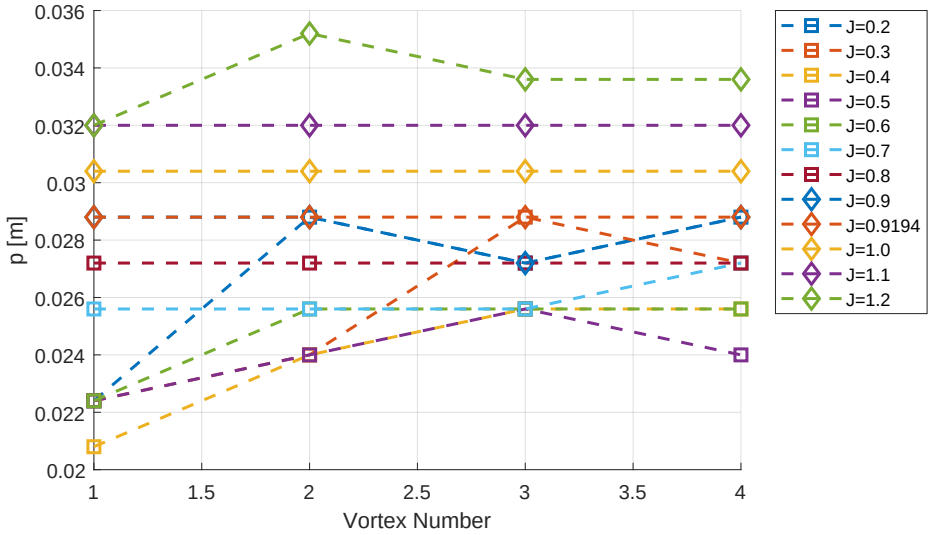

Figure 7: Pitch between vortex centers

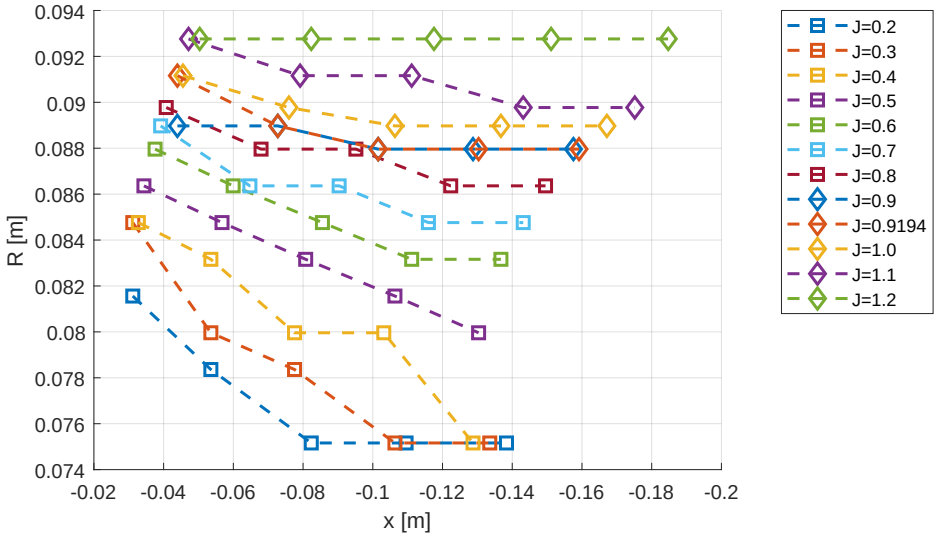

Figure 8: Vortex center radii as function of x coordinate and advance coefficient

5. CONCLUSION AND FUTURE RESEARCH

The vector field and its derivatives were extracted from a set of CFD simulations of a marine propeller. The present post processing methodology was then developed in order to provide tools which improve the understanding of the tip vortex mechanism and its evolution through the propeller wake. Rotational effects were compared by velocity gradient vectors λ_2 and Q. Aiming to identify the five first vortex center on a two-dimensional section plane, two different approaches were used: the search of local pressure minimum and the local deducted velocity minimum, which is the subtraction of advance velocity from the velocity vector field in the longitudinal component. The spiral radius and pitch were defined and calculated, making possible a quantitative comparison of these vortex aspects varying the advance coefficient and center identification approach. Finally, a comparison of the radius evolution in the longitudinal coordinate was presented for various advance coefficients.

This research is part of a numerical and experimental development in marine propulsion, and will provide additional knowledge on the Mod5 series. In the future, the procedure may be applied to PIV results, enabling the validation of the CFD velocity field and its derivatives.

6. ACKNOWLEDGEMENTS

The authors would like to offer our special thanks to the Diretoria de Desenvolvimento Nuclear da Marinha, the Centro Tecnológico da Marinha em São Paulo, the Centro Industrial Nuclear de Aramar, the Instituto de Pesquisas Tecnológicas

do Estado de São Paulo and the Fundação de Apoio ao Instituto de Pesquisas Tecnológicas (FIPT) for the support in the realization of this work.

7. REFERENCES

Banks, D.C. and Singer, B.A., 1995. "A predictor-corrector technique for visualizing unsteady flow". *IEEE Transactions on Visualization and Computer Graphics*, Vol. 1, No. 2, pp. 151–163. ISSN 1077-2626. doi:10.1109/2945.468404.

Esteves, F.R., Gomes, G.G., Katsuno, E.T. and Dantas, J.L.D., 2018. "Simulation of darpa suboff model propeller hull interaction". In *Proceedings of the 27th International Congress on Waterborne Transportation, Shipbuilding and Offshore Constructions*.

Felli, M. and Falchi, M., 2018. "Propeller wake evolution mechanisms in oblique flow conditions". *Journal of Fluid Mechanics*, Vol. 845, pp. 520–559.

Holmén, V., 2012. "Methods for vortex identification".

Jeong, J. and Hussain, F., 1995. "On the identification of a vortex". *Journal of Fluid Mechanics*, Vol. 285, p. 69âĂŞ94. doi:10.1017/S0022112095000462.

Kopp, G., Arenas, A., Ferre-Giné, J. and Girault, F., 2000. "Recent developments in pattern recognition approaches for eddy identification". *ERCOFTAC*, , No. 46, pp. 7–12.

Lesieur, M., Begou, P., Comte, P. and Métais, O., 2000. "Vortex recognition in numerical simulations". *ERCOFTAC*, , No. 46, pp. 25–28.

Lugt, H.J. and Gollub, J.P., 1985. "Vortex flow in nature and technology". *American Journal of Physics*, Vol. 53, No. 4, pp. 381–381. doi:10.1119/1.14177. URL `https://doi.org/10.1119/1.14177`.

Pemberton, R., Turnock, S., Dodd, T. and Rogers, E., 2002. "A novel method for identifying vortical structures". *Journal of Fluids and Structures*, Vol. 16, No. 8, pp. 1051 – 1057. ISSN 0889-9746. doi:https://doi.org/10.1006/jfls.2002.0462. URL `http://www.sciencedirect.com/science/article/pii/S0889974602904627`.

Sbragio, R., 1995. *Projeto Racional de Propulsores de Alto Skew [High Skew Propeller's Rational Design]*. Ph.D. thesis, Universidade de São Paulo, São Paulo, Brazil.

Sbragio, R., 1996. "Modelagem simplificada da cavitação devido à formação de vórtices de ponta em pás de propulsores. [simplified modeling of the cavitation for the tip vortex formation in propeller blades]." In *XVI Congresso Nacional de Transportes Marítimo e Construção Naval, Sociedade Brasileira de Engenharia Naval. pp 77-86.* Rio de Janeiro, Brazil.

Silva Jr, H.C., Esteves, F.R., Dantas, J.L.D., Moura, A.J.S., Neto, W.N.B., Kogishi, A.M. and Sbragio, R., 2019. "Experimental and numerical analysis of tip vortex of a darpa suboff auv propeller". In *Proceedings of the 14th Practical Design of Ships and Other Floating Structures - PRADS 2019 (expected)*. Yokohama, Japan.

Souders, W.G. and Platzer, G.P., 1981. "Tip vortex cavitation characteristics and research and development delay of inception on a threedimensional hydrofoil".

8. RESPONSIBILITY NOTICE

The author is the only responsible for the printed material included in this paper.